NeuroReport 5, 2289–2294 (1994)

Segregation of computations underlying perception of motion discontinuity and coherence

Lucia M. Vaina,[1,2,5,CA]
Norberto M. Grzywacz[2] **and Ron Kikinis**[3]

[1]Boston University, Intelligent Systems
Laboratory, Departments of Biomedical
Engineering and Neurology ERB-331,
44 Cummington St, Boston, MA 02215;
[2]Center for Computational and Biological
Learning, Massachusetts Institute of
Technology, E25-213, 25 Carlton St, Cambridge,
MA 02139; [3]Smith Kettlewell Eye Research
Institute, 2232 Webster St, San Francisco,
CA 94115; Brigham and Women Hospital,
[4]Surgical Planing Laboratory; and [5]Department
of Neurology, Harvard Medical School,
75 Francis St, Boston, MA 02115, USA

[1,CA] Corresponding Author and Address

MOTION is one of the most important cues for detecting discontinuities in images. The major dichotomy among theories of motion-defined discontinuity concerns whether the computations related to the extraction of discontinuity and large scale integration of motion signals are organized hierarchically or occur simultaneously in the brain. In this study we investigated the hierarchical nature of these computations using data from two patients with unilateral brain lesions on two psychophysical tasks: one requiring motion for spatial integration of direction in a stochastic motion field, and the other requiring motion to extract discontinuities in the same type of stimuli. The results showed a surprising double dissociation of deficits on these motion tasks which suggests that models for discontinuity detection requiring a single neural substrate for computing coherence and discontinuity are unlikely to be applicable to the human visual system. We discuss the computational implications of these results. Using morphometric three-dimensional reconstructions of the lesions from the magnetic resonance imaging data we suggest possible anatomical sites mediating these computations.

Key words: Figure–ground segregation; Motion-discontinuity; Motion-coherence; Parietal–temporal lesions

Introduction

The detection of discontinuities in an image underlies the extraction of object borders, breaking of camouflage, identification of objects and other computations important for an animal's survival. Image discontinuities can be discriminated on the basis of difference in luminance, color, disparity, or texture. However, even when these differences are absent discontinuities can easily be perceived as a result of motion.[1–5] Despite the importance of extracting discontinuity the visual measurements that underlie it are still unclear.

Several investigators have studied the theoretical problem of finding motion discontinuities and its relationship to how the visual system measures velocity[6–7] and integrates motion signals over space and time.[8–9] The major dichotomy among these theories concerns whether the computations related to the extraction of discontinuity and large scale integration of motion signals are organized hierarchically or occur simultaneously in the brain.

To address this problem we show here data on two psychophysical motion tasks from two patients A.M.G. and F.D. who suffered a unilateral embolic stroke. One task requires motion for spatial integration of direction in a stochastic motion field and the other requires motion for extracting discontinuities in the same type of stimuli. The patients' performance on other psychophysical motion and static-control tasks was evaluated in detail, and they underwent neurological, neuro-ophthalmological, neuropsychological and neuroradiological examinations. Visual acuity with correction glasses and eye movements were normal, as were temporal frequency and contrast sensitivity for the detection and discrimination of static or moving gratings for stimuli presented in either visual field. The patients' performance on tasks of form, texture and color discrimination was also normal.

Patients

Patient A.M.G. is a 52-year-old right-handed woman who had a lesion in the left hemisphere in the occipital–parietal area. Figure 1A shows the lesion in three-dimensional morphometric reconstruction of the brain, derived from the magnetic resonance image data by combining semiautomated segmentation with manual editing. The lesion on the surface of the brain (Figure 1B) involves Brodmann's areas 19 and 39 and medially area 18. Figure 1C shows that a large part of the lesion occurs deep in the occipital white matter. On neurological examination A.M.G. had no motor defi-

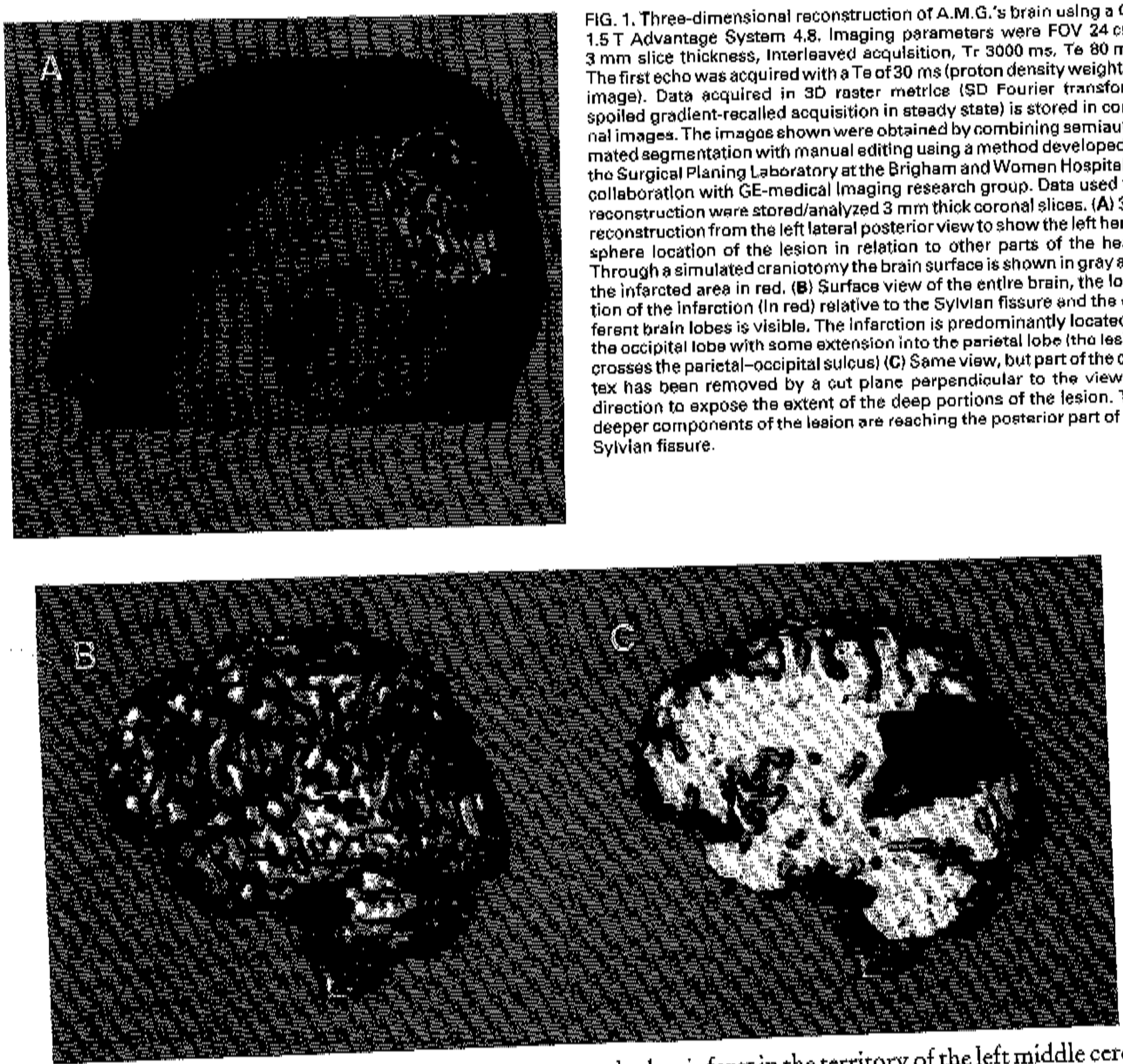

FIG. 1. Three-dimensional reconstruction of A.M.G.'s brain using a GE 1.5 T Advantage System 4.8. Imaging parameters were FOV 24 cm, 3 mm slice thickness, interleaved acquisition, Tr 3000 ms, Te 80 ms. The first echo was acquired with a Te of 30 ms (proton density weighted image). Data acquired in 3D raster metrice (3D Fourier transform spoiled gradient-recalled acquisition in steady state) is stored in coronal images. The images shown were obtained by combining semiautomated segmentation with manual editing using a method developed in the Surgical Planing Laboratory at the Brigham and Women Hospital in collaboration with GE-medical Imaging research group. Data used for reconstruction were stored/analyzed 3 mm thick coronal slices. (A) 3-D reconstruction from the left lateral posterior view to show the left hemisphere location of the lesion in relation to other parts of the head. Through a simulated craniotomy the brain surface is shown in gray and the infarcted area in red. (B) Surface view of the entire brain, the location of the infarction (in red) relative to the Sylvian fissure and the different brain lobes is visible. The infarction is predominantly located in the occipital lobe with some extension into the parietal lobe (the lesion crosses the parietal–occipital sulcus) (C) Same view, but part of the cortex has been removed by a cut plane perpendicular to the viewing direction to expose the extent of the deep portions of the lesion. The deeper components of the lesion are reaching the posterior part of the Sylvian fissure.

cits, she had a mild anomia, slight short term memory loss and difficulties with spelling and calculations. Neuro-ophthalmological examination revealed a minor right inferior quadranopsia for small stimuli. The patient's major complaint was that 'I almost don't see how things are moving'. Consistent with her complaint, formal psychophysical testing showed her perception of local motion stimuli presented in the right visual field (contralateral to her lesion) to be severely impaired. Specifically, when presented with random dot cinematograms in which dots took independent two-dimensional random walks, she could not discriminate between moving displays that differed fivefold in speed. Moreover, the maximum spatial offset over which she could detect a coherent displacement of random dots (D_{max}) was half that of the normal controls. She was also severely impaired on identifying a two-dimensional figure or letter from the background using motion cues alone (speed or direction). Her performance on all these motion tasks was normal for stimuli presented in the left visual field.

Patient F.D. is a 42-year-old right-handed man who had an infarct in the territory of the left middle cerebral artery. Figure 2 shows a three-dimensional reconstruction of the lesion which involves the left temporal and temporal–parietal areas, involving Brodmann's areas 21, 22, 37 and 39 and just slightly area 19. On neurological examination, F.D. was found to have right-side weakness of both arm and leg and cognitively, he showed word finding difficulties. However, in a few weeks he fully recovered from these deficits. His visual fields were full. The patient complained about his difficulties in coping with interfering noise, visual or auditory. In contrast with A.M.G.'s impaired performance on a large set of motion tasks (listed above) F.D.'s performance was normal on these tasks for stimuli presented in either visual field.

Methods and Results

The two major motion tasks employed dynamic random-dot patterns in which a varying proportion of the dots provided a correlated motion signal spatially dispersed in masking noise. The signal dots jumped from

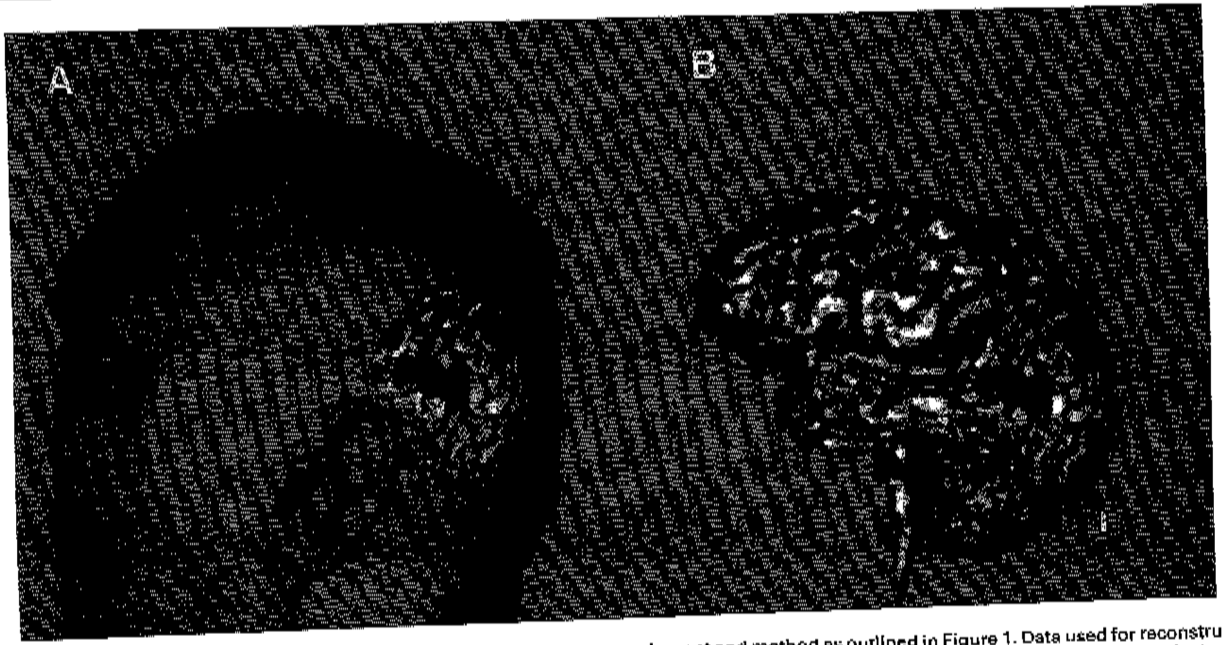

FIG. 2. Three-dimensional reconstruction of F.D.'s brain using the same equipment and method as outlined in Figure 1. Data used for reconstruction was stored/analyzed as 124 1.5 mm thick coronal slices. (A) 3-D reconstruction from the left posterior view to show the left hemisphere location of the lesion to other parts of the head. Through simulated craniotomy the brain surface is shown in gray and the infarcted area in red. (B) View of the lateral surface of the brain. The infarction (in red), relative to the posterior part of the superior temporal sulcus involves the temporal and, slightly, the temporo–parietal region.

frame to frame with constant step size while noise dots were plotted in each frame at random locations within the stimulus aperture. To vary the strength of the motion signal the stimuli were displayed using an adaptive staircase procedure. In both tasks described here the stimulus subtended 79°.[2] The motion-coherence display (Fig. 3A) was similar to that used by Newsome and Paré[10] and in our previous studies.[11,12] A four alternative forced-choice procedure (up, down, left, or right) was used to measure threshold, defined as the average of the last nine reversals in the staircase. In the motion-discontinuity task, the stimuli characteristics and test procedure were identical to those of the motion-coherence experiment except that in half of the trials an illusory line divided the display into two equal parts (Fig. 3B) and in others the display was homogeneous. This illusory line was entirely defined by the difference in the direction of motion of the coherent signal dots on the two sides of the boundary. In both types of display the signal dots moved coherently vertically, either upwards or downwards. Threshold, obtained using a two-alternatives forced choice procedure indicated the proportion of signal dots for which observers could successfully discriminate between homogeneous and discontinuous displays. To prevent the use of spatial local cues, the illusory line had four possible orientations (vertical, horizontal, or oriented 45° to the right or left of the vertical) and its center was slightly offset from the center of the aperture (the amount of offset randomly varied, but in all cases it remained within 0.5° from the center of the circular aperture).

Subjects sat 60 cm from a monochrome computer display. Testing was conducted in a quiet dark room and each session began with 15 practice trials and feedback on wrong responses, after which feedback was no longer provided. Subjects were instructed to fixate a small black fixation mark situated at 2° to the left or right imaginary border of the stimulus. Informed consent according to Boston University Human Subjects Committee was obtained from all the subjects included in the study. Figure 3B shows the results of the motion-coherence task for the two patients and 23 control subjects. A.M.G.'s performance on this task was normal for stimuli presented in either visual field. In contrast, F.D. was impaired for stimuli presented in his right hemifield ($p < 0.05$). Figure 3D shows results from the motion-discontinuity task for the two patients and 16 normal control subjects. A.M.G.'s performance for stimuli presented in the right visual field was significantly worse ($p < 0.001$) than her performance for stimuli presented in the left visual field, which was normal, and the performance of normal control subjects. Her impaired performance did not correlate with the specific orientations of the imaginary motion discontinuity line, thus A.M.G.'s small visual field loss in the lower right quadrant cannot account for this deficit. F.D.'s performance on this task was normal.

To determine whether F.D.'s deficit on the motion-coherence test was an indication of a failure to discriminate direction in a noisy motion display or a deficit of assessing coherence, we conducted a control task. In this task the stimulus consisted of two circular apertures displayed simultaneously one above the other

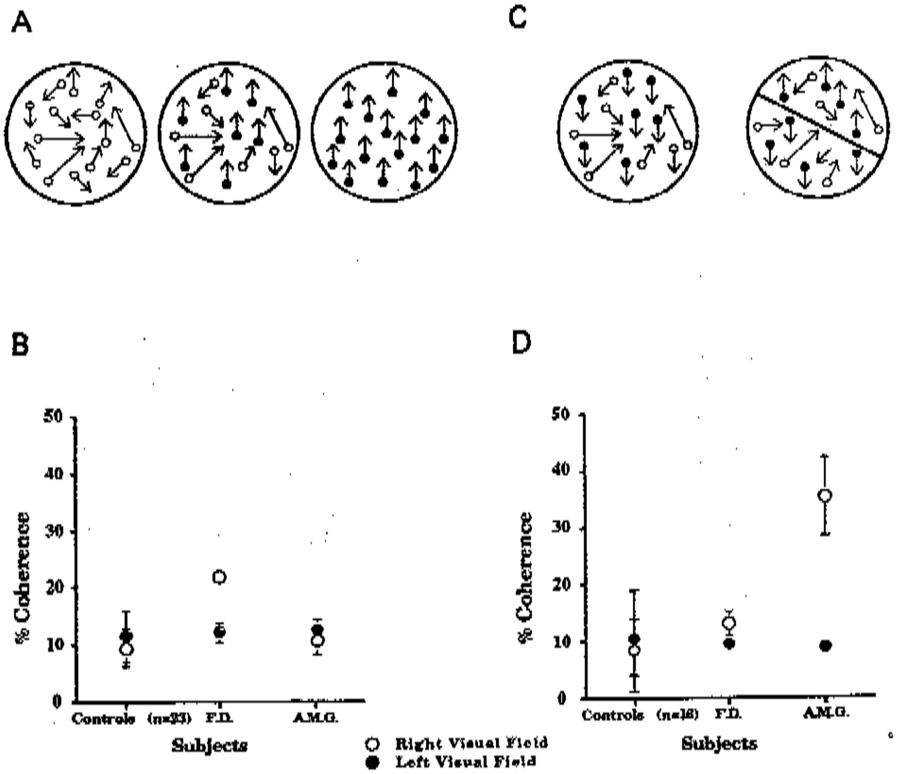

FIG. 3. **(A)** A schematic representation of the random dot stimuli used in this experiment.[12] Each dot survived for a brief period of time before being replaced. In the 100% correlation on the right each dot was replaced by a dot with a constant offset in space and time. In the 0% correlation on the left the dots were plotted in each frame at random locations within the display. In the middle case, 50% correlation, a specifiable percentage of the dots carried the correlated motion signal while the remaining dots were dynamic masking random noise. **(B)** The results on the motion coherence task from A.M.G., F.D. and 23 normal control subjects. A.M.G. and F.D.'s data resulted from the averaging of three thresholds obtained on three non-consecutive days, but no more than one week apart. Error bars show ± s.e. **(C)** Schematic illustration of the dynamic random dot motion stimuli employed in the motion-discontinuity task. The motion of signal dots was always vertical, and in the trials where motion defined boundary was present the two directions were always opposite. **(D)** The results on the motion-discontinuity test from 16 control subjects and A.M.G. and F.D. The patients' data plotted here resulted from averaging three thresholds obtained on three non-consecutive days, but no more than one week apart. Error bars show ± s.e.

with 8° distance between their centers and each subtending roughly 28°.[2] In one, randomly located on the top or the bottom, a staircase procedure was used to vary the proportion of directionally coherent signal dots, and in the other aperture only noise dots were displayed. The subject's task was to first choose the aperture which contained the mixture of signal and noise dots, and then to determine the direction of the signal dots. On this task F.D. needed the same proportion of signal dots as in the one aperture motion-coherence test, which indicates that his deficit was one of detecting coherence at low correlation levels, and not of direction discrimination. Similar to her performance on the motion-coherence task, A.M.G.'s performance was normal on this task.

Discussion

Implications of the experimental results for theories of motion discontinuity: It could be argued that A.M.G.'s deficit on the motion-discontinuity task may not be due to a failure of detecting motion signal gradients embedded in noise, but rather a deficit of spatial integration. This would suggest that she needs a larger integration area than observers with normal performance. Because each half of the motion-discontinuity display (Fig. 3B) is only half of the area of the motion-coherence display (Fig. 3A), the motion signals available to A.M.G. might have been below her thresholds of integration. However, since her performance on the motion-coherence experiment was normal for a display with a smaller aperture (roughly 28°^{2}) than that of each half of the motion-discontinuity display (> 39°^{2}), this possibility is ruled out.

The dissociation between the computations of motion-discontinuity and large-scale motion-coherence (Fig. 3B and D) raises the following question: given that to see the motion in each half of the motion-discontinuity display one must integrate its signals to overcome the noise, how is it possible that patients who require a high percentage of coherent motion signal in the motion-coherence task, like F.D., perform normally in the motion-discontinuity task?

A likely answer is that the process of discontinuity detection involves a form of motion integration different from that used to discriminate direction in the motion-coherence task. To detect boundaries, the area of integration should be small. Certainly, it must be much smaller than the area used in our motion-coherence displays. One possibility for the integration in the detection of motion discontinuity is that directionally selective cells with strong surround inhibition compute discontinuity.[13–15] In this case, there would be spatial integration within the receptive field center of such cells. Another possibility is the detection of a bimodal distribution of motion energy signals at the border when using direction of motion as the dependent variable.[16,17] This detection requires the integration of information over a finite area so that the statistics necessary to detect the bimodal distribution are reliable.[18]

From the conclusion that the area of integration involved in detecting motion discontinuity is small it follows that adaptive models for discontinuity detection such as that proposed by Koch *et al*[19] are unlikely to be applicable to the human visual system. These models predict that the scale of motion spatial integration is as large as the area surrounded by the discontinuities. For instance, Koch *et al* show that their model accounts for the large-scale phenomena of motion capture and motion coherence.[19] In this model the integration is achieved through Markov random fields and the discontinuity is detected by line processors. Roughly, this theory postulates the existence of two sets of cells. The first set, which we call the Markov set, tries to compute a coherent-motion field by minimizing differences in motion signal between neighboring cells. Simultaneously, the other set, the line-processor set, measures whether the signal difference between neighboring cells in the Markov set is larger than a given threshold. If it is so, the line-processor set sends inhibitory signals to interrupt the flow of information between the dissenting cells in the Markov set. Such a mechanism would predict that if the computation of coherence is impaired, then so is the computation of discontinuity. In this case, the Markov set would be damaged and thus would not provide sufficient information for the line-processor set to work.

An alternative to adaptive models for discontinuity that is consistent with our presented data is schematically illustrated in Figure 4. Basic motion measurements (for example, directional, temporal, and probably speed signals) feed in parallel into two mechanisms: one devoted to the computation of discontinuities and the other devoted to motion coherence. As discussed above, the discontinuity mechanism would also integrate the basic motion measurement although with a smaller scale than the motion-coherence mechanism. The discontinuity mechanism would provide border information for the coherence mechanism to set boundary conditions for its spatial integration. (The alternative scheme that large-scale coherence computation precedes discontinuity computation is unlikely, since the discontinuities would be smoothed out too soon.) Both the coherence and discontinuity information would be accessible by higher level computations. Under this scheme, if the motion-coherence mechanism is damaged, then the observer may still detect the discontinuity. By the same token, if the motion-discontinuity mechanism is damaged, then the observer may perceive coherent motion.

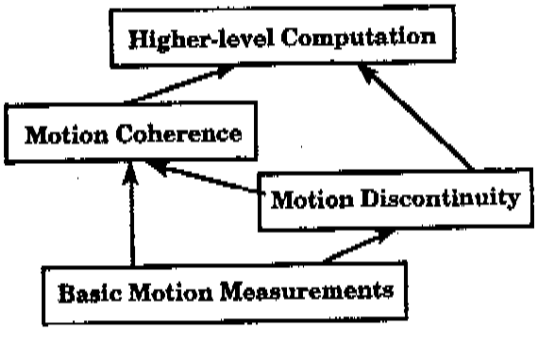

FIG. 4. Theoretical framework for the organization of the computations of motion discontinuity and coherence. The first stage obtains basic local motion measurements, such as the direction of motion, local spatial and temporal frequencies, and perhaps speed. This stage sends this information to a stage that computes motion discontinuities. Both the discontinuity and basic motion measurement information are transmitted to the motion coherence stage, where the basic motion information is integrated within boundaries computed by the discontinuity stage. The high level motion centers have access to both the coherent information and the discontinuities. In this case, damage to the coherence stage does not impair detection of discontinuities and *vice versa*.

Speculations on functional–anatomical correlates of the discontinuity and coherence mechanisms: If the scheme Figure 4 is correct, one would expect that the computations involved in discontinuity detection and large-scale motion integration are mediated by globally different cortical areas of the brain, unless two very different mechanisms are inextricably mixed, yet can be selectively damaged by cerebrovascular accidents.

Because we have detailed neuroimaging data on A.M.G. and F.D. and because we studied in detail both patients' visual motion perception abilities, it is natural to speculate on the likely anatomical substrate for these computations. Figure 2 shows that F.D.'s lesion is almost entirely cortical and by and large involves the posterior portion of the temporal lobe. It appears, however, that the lesion involved the cortical area at the confluence of Brodmann areas 19 and 37 inferiorly, which was postulated as the putative human homologue of the macaque MT[12,20,21] that is critical for the analysis of motion-coherence.[10] In contrast, as shown in Figures 1 A.M.G.'s lesion substantially involves the white matter in the occipital–parietal region and cortically the Brodmann areas 19, 39 and medially 18. The latter might be a good candidate for mediating the computation of motion discontinuities.[22] Another possibility are a class of neurons in MT (specifically MT_{α}) and ventral MST which are involved in computing the location of motion discontinuity in the visual field.[15] It is possible that at least one of these areas was involved directly or indirectly in A.M.G.'s lesion.[23] Functionally, her speed and direction discrimination deficits, together with her deficits on figure–ground separation by motion cues are consistent with the putative involvement of these areas in her lesion. But if an impairment of MT_{α} underlies the discontinuity deficit, then F.D.'s normal performance on this task implies that his MT lesion must not include MT_{α}. Indeed, F.D.'s normal performance on several other motion tasks known to be mediated by population of neurons in MT, suggests that this area was probably only partially involved in his lesion.

Conclusion

Our finding of a double dissociation between the computations of motion-discontinuity and large-scale motion-coherence presented in this study, suggests a computational and anatomical segregation of these mechanisms. This conclusion reinforces the view[24–26] that the human motion system is not organized in a simple linear hierarchy, but as converging and diverging parallel pathways.

ACKNOWLEDGEMENTS: We thank Alan Cowey and an anonymous reviewer for useful suggestions on the manuscript and Thomas Kemper for advice on the anatomical localization of the patients' lesions. This research was supported by NIH grant EY-RO1–07861, McDonnell-Pew Foundation Grant T89-01245-017, and ONR contract N00012-93-1 to L.M.V. and AFOSR contract F49620-92-J0256 to N.M.G.

Received 5 August 1994;
accepted 2 September 1994

References

1. Anatis SM. *Vision Res* **10**, 1411–1430 (1970).
2. Julesz B. *Foundation of Cyclopean Perception*. Chicago: University of Chicago Press, 1971.
3. Baker CL and Braddick OJ. *Vis Res* **22**, 851–856 (1982).
4. Regan D, Beverley KI. *J Opt Soc Am A* 433–442 (1984).
5. Vaina LM, Grzywacz NM. Testing computational theories of motion discontinuities: a psychophysical study. In: Sandini G, ed. *Lecture Notes in Computer Science*, **588** Springer-Verlag, 1992: 212–216.
6. Nakayama N and Loomis JM. *Perception* **3**, 63–80 (1974).
7. Grzywacz NM and Yuille AL. *Proc R Soc Lond* **239**, 129–161 (1990).
8. Hildreth EC. *The Measurement of Visual Motion*. Cambridge: MIT Press. 1984.
9. Bulthoff HB, Little J and Poggio T. *Nature* **337**, 529–553 (1989).
10. Newsome WT and Paré EB. *J Neurosci* **8**, 2201–2211 (1988).
11. Vaina LM, Stratton NA *et al. Invest Ophthal Vis Sci* **32** (Suppl.), (1991).
12. Vaina LM, LeMay M, Bienfang DC *et al. Vis Neurosci* **5**, 353–371 (1990).
13. Frost DJ and Nakayama K. *Science* **220**, 744–745 (1983).
14. Allman J, Miezin F and McGuinness E. *Perception* **14** 105–126 (1985).
15. Tanaka K, Hikosaka K *et al. J Neurosci* **6**, 134–144 (1986).
16. Grzywacz NM, Smith JA and Yuille AL. *Proc IEEE Workshop Vis Motion*, 148–155 (1989).
17. Spoerri A and Ullman S. *Proc Int Conf Computer Vision*, 209–216 (1987).
18. Vorhees H and Poggio T. *Nature* **333**, 364–367 (1988).
19. Koch C, Wang HT and Mathur B. *J Exp Biol* **146**, 115–139 (1989).
20. Zeki S. *Brain* **114**, 811–824 (1991).
21. Watson JDG *et al. Cerebral Cortex* **1**, 79–94 (1993).
22. Lagae L, Gulyas B, Raiguel S *et al. Soc Neurosci Abstr* **14**, 457 (1988).
23. Maunsell JHR and van Essen DC. *J Neurosci* **3**, 2563–2586 (1983).
24. Nakayama K. *Vis Res* **25**, (1985).
25. Wilson HR, Ferrera VP and Yo C. *Vis Neurosci* **9**, 79–97 (1992).
26. Merrigan W and Maunsell JH. *Ann Rev Neurosci* **16**, 369–402 (1993).
27. Nakayama K and Tyler CW. **21**, 427–433 (1981).
28. Vaina LM, Grzywacz NM and Kikinis R. *Invest Ophthal Vis Sci* **34** (Suppl.) 1033 (1993).